Angular distributions in multifragmentation

R. W. Stoenner, R. L. Klobuchar, P. E. Haustein, G. J. Virtes, and J. B. Cumming*
Chemistry Department, Brookhaven National Laboratory, Upton, New York 11973, USA

W. Loveland
Department of Chemistry, Oregon State University, Corvallis, Oregon 97331, USA
(Received 9 January 2006; published 7 April 2006)

Angular distributions are reported for ^{37}Ar and ^{127}Xe from 381-GeV ^{28}Si + Au interactions and for products between ^{24}Na and ^{149}Gd from 28-GeV ^{1}H + Au. Sideward peaking and forward deficits for multifragmentation products are significantly enhanced for heavy ions compared with protons. Projectile kinetic energy does not appear to be a satisfactory scaling variable. The data are discussed in terms of a kinetic-focusing model in which sideward peaking is due to transverse motion of the excited product from the initial projectile-target interaction.

DOI: 10.1103/PhysRevC.73.047602 PACS number(s): 25.70.Pq, 25.75.−q, 25.40.Ve, 25.70.Mn

Multifragmentation (MF) was observed [1] shortly after protons were accelerated to multi-GeV energies. Copious yields of intermediate mass fragments (IMFs) such as ^{18}F and ^{24}Na from heavy element targets appeared inconsistent with those expected from deep spallation or binary fission mechanisms. The power-law dependence of yield on fragment mass [2,3] suggested a multiparticle breakup associated with liquid-gas phase transitions in excited nuclear matter. The possibility that MF could probe the thermodynamics of nuclear matter provided impetus for numerous studies of MF induced by energetic proton and heavy ions; see the reviews by Moretto and Wozniak [4] and by Richert and Wagner [5]. Recent work includes the derivation of caloric curves for and the phase diagram of finite nuclear matter [6,7].

A two-step picture of MF entails an initial projectile-target interaction leading to some moving configuration of hot, possibly compressed nuclear matter. In step two, thermal expansion, with decompressional flow in the case of heavy-ion-induced MF, moves the system into a phase region of spinodal instabilities where excited prefragments form. After freeze-out, these are further accelerated by Coulombic forces and may de-excite by particle emission to give the observed IMFs. For details, see the review by Chomaz, Colonna, and Randrup [8]. Significant fragment-fragment interactions occur after what are normally considered freeze-out densities [9].

An interesting feature of MF is the onset of sideward-peaked angular distributions at high energies [10,11]. The transition from forward to sideward peaking occurs for protons between 3 and 11 GeV [12]. Some distributions peak at angles slightly greater than 90° for still higher energies [12,13]. Mechanisms such as nuclear shock waves [10] or exotic geometries for the excited intermediate [14–17] have been proposed. Transverse momentum transfer in the initial interaction might also lead to sideward-peaked angular distributions [18,19].

Previous work from this laboratory [20,21] reported that the angular distribution of an IMF, ^{37}Ar, from Au shifted from forward peaked for incident 8-GeV ^{22}Ne ions to peaked near 90° for 25-GeV ^{12}C. This report extends those measurements to a higher energy, 381-GeV ^{28}Si from the Brookhaven AGS. By-products of these studies are angular distributions for ^{127}Xe, a deep-spallation product. Experimental procedures were identical to those used previously: ^{37}Ar and ^{127}Xe recoils from 200-μg/cm^2 Au targets were extracted by melting the Al catcher foils in the presence of carrier Ar and Xe and were purified by gas chromatography. The results of these measurements are compared with the lower energy distributions in Fig. 1. General trends are shown by fits to cubic polynomials in $\cos\theta_{\mathrm{lab}}$.

The distribution for ^{37}Ar at 8 GeV in Fig. 1 exhibits a broad forward peak. However, the pronounced downward concavity suggests a sideward component. As the projectile energy increases to 25 GeV the distribution "tilts" and a peak near 90° becomes apparent. Although the integrated F/B ratio of the distribution is 1.00 ± 0.02, the intensity ratio $F(0°)/F(180°)$ is less than unity. This small-angle deficit and the ^{37}Ar distribution are comparable to those reported for Sc isotopes from 400-GeV-proton-induced MF of U [12].

The ^{37}Ar distribution from 381-GeV ^{28}Si + Au is further shifted backward. The integrated F/B has decreased to 0.73 ± 0.08, confirming the enhanced "backsplash" inferred from the thick-target, thick-catcher measurements with 232-GeV ^{16}O ions [22]. A 2π thick-catcher experiment with a 100-μg/cm^2 target gave an F/B of 0.76 ± 0.05, in agreement with that from the angular distribution at 381 GeV.

Foward peaking of the angular distributions for ^{127}Xe in Fig. 1 decreases as the projectile energy increases. The distribution at 381 GeV is nearly identical to that for ^{37}Ar at 8 GeV. Whether the ^{127}Xe distribution would continue to shift backward for still higher energies is an open question. The distribution of ^{128}Ba from p + U does shift from forward to sideward peaked between 3 and 11.5 GeV [23].

Some distortion of the angular distributions of ^{127}Xe by scattering and/or absorption in the targets was expected owing to the short ranges of deep-spallation products [24]. To achieve high collection efficiency, recoil paths as long as 500 μg/cm^2 were accepted at some angles. The influence of target thickness

*Electronic address: cumming@bnl.gov

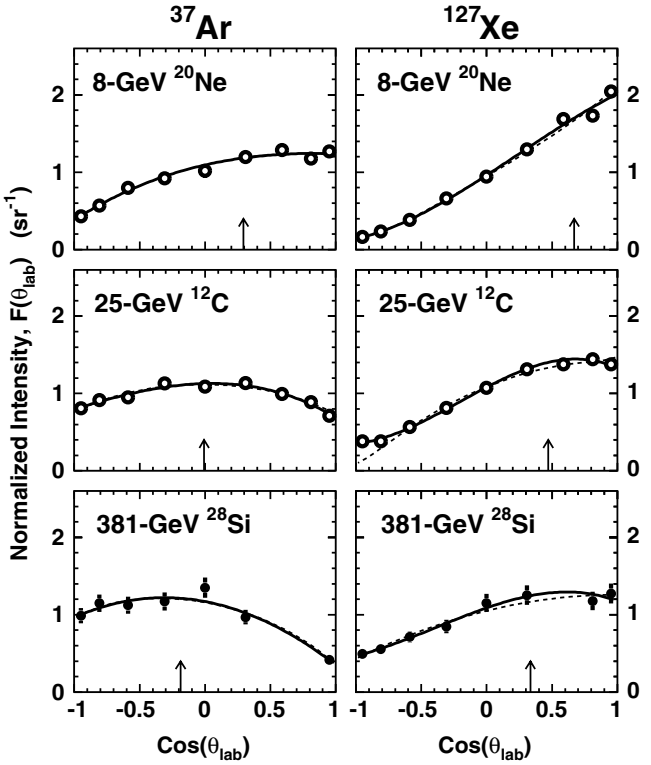

FIG. 1. Angular distributions of ^{37}Ar and ^{127}Xe from the fragmentation of Au by heavy ions. Filled points are from the present work; open ones are from Refs. [20,21]. Solid curves are normalized cubic polynomials in $\cos\theta_{\rm lab}$; dashed ones are fits to a kinetic focusing model. Arrows indicate the direction of the cascade recoil (see text).

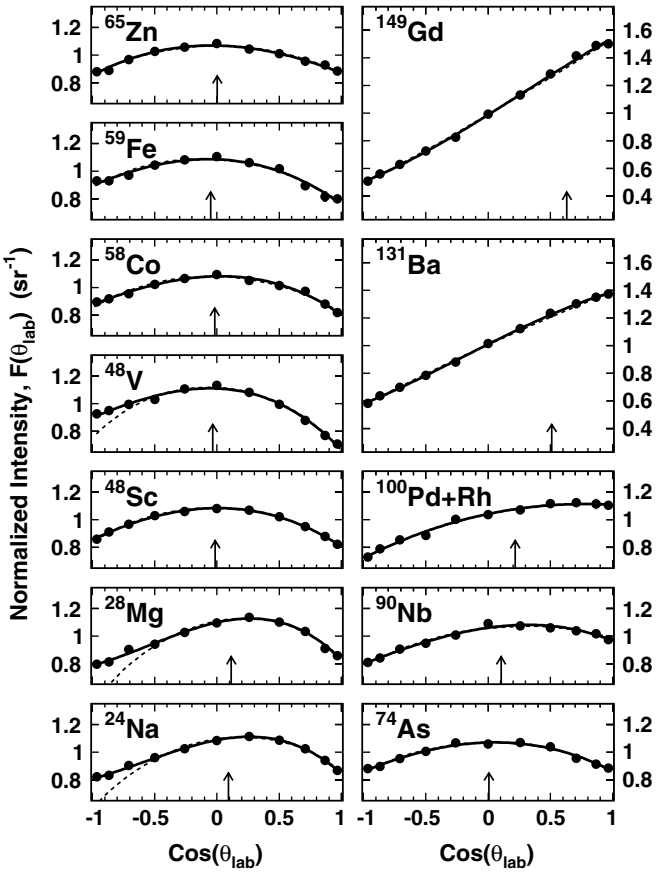

FIG. 2. Angular distributions for products of the fragmentation of Au by 28-GeV protons. Solid curves are normalized cubic polynomials in $\cos\theta_{\rm lab}$; dashed ones are fits to a kinetic focusing model. Arrows indicate the direction of the cascade recoil (see text).

was studied in measurements with 28-GeV protons in which angular distributions were obtained with a low collection geometry (0.5% of 4π sr). A variety of products were assayed by γ-ray spectroscopy of the Mylar catcher foils. Experiments with a forward (F) target orientation (normal at 45° to the beam) covered angles from 15° to 105° for 100-, 200-, and 500-μg/cm^2 Au targets. Three others with a backward (B) orientation (normal at 135°) spanned the range from 75° to 165° for one 100- and two 200-μg/cm^2 targets. Angular distributions for all products with $A \leqslant 100$ were independent of target thickness. A significant dependence was observed for nuclides with $A \geqslant 131$ at angles where recoil paths in the target were long: at 90° and 105° for the F orientation and at 75° and 90° for B. For these products, effects increased with increasing fragment mass but saturated as the distributions were unchanged above 200 μg/cm^2. We conclude that the angular distributions for ^{37}Ar in Fig. 1 are not distorted by the 200-μg/cm^2 targets but those for ^{127}Xe are. Because of different target and collection geometries from the proton experiments, it was not practical to correct the ^{127}Xe data.

The variety of shapes encountered in the fragmentation of Au by 28-GeV protons is illustrated by the target-thickness-corrected angular distributions in Fig. 2. Those for fragments with A = 48–74 are nearly symmetric about 90°, with a tendency for small deficiences at the most forward angles. This backsplash is most pronounced for the neutron-deficient ^{48}V. It is significantly lower for the isobaric ^{48}Sc. Distributions in this mass region are similar to those reported for Sc isotopes from the interaction of 400-GeV protons with U [12].

Distributions for ^{24}Na and ^{28}Mg in Fig. 2 shift forward from 90° and are skewed compared with those for A = 48–74. Data [10] for fragments with Z = 6–12 indicate that this evolution continues for still lower mass IMFs. There is also a shift to forward peaking as fragment mass increases above A = 74. Distributions for ^{131}Ba and ^{149}Gd are strongly forward peaked. Angular distributions from U targets do not show this transition. Sideward peaking persists at least as far as the Ba isotopes [23].

The $F(0°)/F(180°)$ ratio, a measure of the forward or backward shift of an angular distribution, is shown in Fig. 3 as a function of the projectile energy for IMFs with A = 37−48. A solid curve shows the trend for Sc isotopes (open triangles) from p + U [12]. The open circles for ^{48}Sc and ^{48}V from the present work are consistent with that curve. Similar angular distributions are reported for Sc isotopes from Au and U at 400 GeV [25] and for Z = 6–12 nuclides at 28 GeV [10]. The downturn below 3 GeV may indicate the transition to a binary mechanism [26,27].

Values of $F(0°)/F(180°)$ for ^{37}Ar from HI-induced MF of Au are shown as filled circles in Fig. 3. It has been suggested that projectile energy is the appropriate variable for comparing

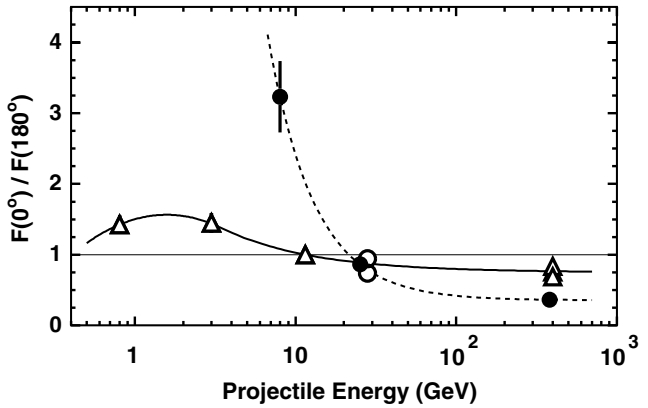

FIG. 3. The 0° to 180° intensity ratio as a function of projectile energy for MF reactions yielding products with $A = 37$–48. Open triangles are from Ref. [12] for Sc isotopes produced in p + U interactions. A solid curve indicates their trend. Open circles are for p + Au $\rightarrow {}^{48}$Sc and ^{48}V from the present work. Filled circles are for HI + Au $\rightarrow {}^{37}$Ar from the present work and Refs. [20,21]. Their trend is shown by the dashed curve.

angular distributions [28]. Although the solid and dashed curves cross at ∼25 GeV, energy scaling does not appear valid over a wider range. The forward peak is more pronounced at lower energies and the forward deficit is deeper in the limiting fragmentation region for the HIs.

Hsi *et al*. [18,19] have suggested that the shift from forward- to sideward-peaked angular distributions is due to a change in direction of motion of the excited prefragment from the initial projectile-target interaction. They examined a subset of p + Au internuclear cascade calculations (INCCs) for which the excitation energy E^*, of the residue was $\geqslant$500 MeV, typical for IMFs. The mean angle of the residue, θ_{cr}, shifted from ∼30° at 0.6 GeV to ∼79° at 90 GeV. The most rapid growth of the transverse velocity was in the energy region where sideward peaking emerges. They showed that a variety of data from the ISiS experiment (Au + 14-GeV p) are consistent with a kinetic-focusing model (KFM) that combined the INCCs with a statistical multifragmentation model.

The angular distributions in Figs. 1 and 2 were least-squares fitted with a simple form of the KFM to give two parameters, $\eta_\parallel = \langle v_\parallel / V \rangle$ and $\eta_\perp = \langle v_\perp / V \rangle$, for each product. Here $v_\parallel$ and $v_\perp$ are the components of cascade recoil velocity and V is the mean velocity from the subsequent fragmentation step. Results are shown as dashed curves in both figures. This simple model can reproduce a variety of shapes. Many of the fits are indistinguishable from the cubic polynomials. The simple model was unable to reproduce the skewing of the ^{24}Na and ^{28}Mg distributions. Calculated curves for these isotopes excluded $\theta_{lab} \geqslant 135°$. The difference between solid and dashed curves amounts to only 2%–3% of the total events. A similar problem appeared to a lesser extent (<1%) for ^{48}V, but not for the isobaric ^{48}Sc. The model might be improved by inclusion of the broad distributions of $v_\parallel$ and $v_\perp$ predicted by the INCCs.

To facilitate comparisons with the INCCs, $\eta_\parallel$ and $\eta_\perp$ were converted to velocities with the assumptions that $v_\parallel = \eta_\parallel V$ and $v_\perp = \eta_\perp V$. Values of V were obtained from thick-target,

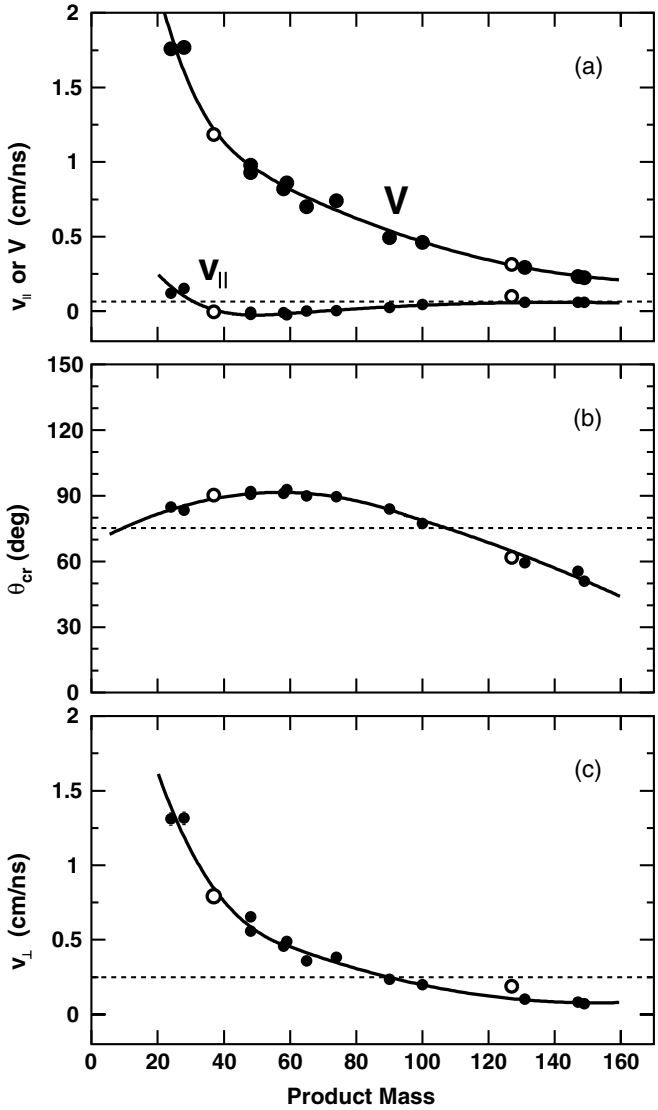

FIG. 4. Dependence of KFM parameters on product mass. Filled points are from the present work for 28-GeV p + Au open ones are from Refs. [20,21] for 25-GeV ^{12}C + Au. Values of V in the uppermost panel were obtained from Ref. [24]. Smooth curves show data trends.

thick-catcher measurements [24]. The dominant trend of V, the upper points in Fig. 4(a), is the decrease with product mass.

Values of $v_\parallel$, $v_\perp$, and the cascade recoil angle θ_{cr} defined by $\tan(\theta_{cr}) = \eta_\perp / \eta_\parallel$ from the p + Au distributions are presented as a function of product mass in Fig. 4. Dashed lines in each panel are mean values from the INCCs for 28-GeV p + Au [18]. The data are not consistent with a single average cascade residue as the intermediate state. Open points for ^{37}Ar and ^{127}Xe from 25-GeV ^{12}C + Au have been included in Fig. 4 to emphasize the similarity of the distributions in this energy region. This does not persist at higher or lower energies. INCCs predict that KFM parameters should depend on the excitation energy E^*, of the cascade residue [19]. Values of $v_\parallel$ for ^{24}Na and ^{28}Mg are above the mean, in Fig. 4(a). Those for products with heavier masses initially drop below the mean but then rise back in the deep-spallation region. The positive

correlation between $v_\parallel$ and E^* [19] suggests that products with $A = 37-74$ are formed, on the average, in lower E^* events than either the lighter IMFs or the deep-spallation products. Flatter excitation functions for the middle mass products [1] support this conclusion.

The direction of motion, θ_{cr}, of the cascade residues from the KFM is shown as a function of product mass in Fig. 4(b). The mean angle from INCCs is 75°. An angular distribution need not peak at θ_{cr} [18]. For example, the KFM fit gives $\theta_{cr} = 59°$ for the strongly forward peaked distribution of ^{131}Ba in Fig. 2. As the projectile energy increases, the calculated curves for ^{127}Xe in Fig. 1 remain forward peaked as θ_{cr} increases from 48° to 70°. A substantial $v_\perp$ for ^{37}Ar production by 8-GeV ^{20}Ne appears as a downward concavity rather than as a peak at $\theta_{cr} = 73°$ in Fig. 1. Sideward peaking begins to emerge at about that value. The extrapolation of the curve below $A = 24$ in Fig. 4(b) is consistent with the known shift to forward-peaked distributions for the lighter MF products [10]. INCCs predict a decrease of θ_{cr} with increasing E^* [19]. Sideward-peaked angular distributions in the $A = 37-74$ region again suggest lower E^* for such products.

An approximately monotonic decrease of $v_\perp$ with product mass is seen in Fig. 4(c). The positive correlation between $v_\perp$ and E^* [19] would then suggest that the lowest E^* values occur in the deep-spallation region, a conclusion at variance with those drawn from $v_\parallel$ or θ_{cr}. Note also that $v_\perp$ values for ^{24}Na and ^{28}Mg are >4 times the INCC mean. The low frequency of such values in the calculations [18] appears inconsistent with the large yields in this region. Although the KFM can describe the various shapes of angular distributions, $v_\perp$ for some of the IMFs is larger than expected from the calculations. A very different model, one that replaces $v_\perp$ with an intrinsic anisotropy of V having the form $(1 + a\cos^2\theta)/(1 + a/3)$, can also fit angular distributions (e.g., see Ref. [12]). This form suggests angular momentum effects on the fragmenting system. In the same manner as θ_{cr} shifted from forward to sideward with increasing energy in p-nucleus collisions [18], the orientation of the angular momentum vector of the cascade residue is expected to shift from perpendicular to the beam in the compound-nucleus regime to more parallel at very high energies. A high-energy p-nucleus collision might look much like an interaction with a transverse-moving lower energy particle. Such an angular momentum effect could augment $v_\perp$ in producing sideward peaking.

This research was supported by the Office of High Energy and Nuclear Physics of the U.S. Department of Energy under Contract Nos. DE-AC02-98CH10886 with Brookhaven National Laboratory and DE-FG06-97ER41026 with Oregon State University.

[1] R. Wolfgang, E. W. Baker, A. A. Caretto, J. B. Cumming, G. Friedlander, and J. Hudis, Phys. Rev. **103**, 394 (1956).
[2] R. W. Minich *et al.*, Phys. Lett. **118B**, 458 (1982).
[3] J. E. Finn *et al.*, Phys. Rev. Lett. **49**, 1321 (1982).
[4] L. G. Moretto and G. J. Wozniak, Annu. Rev. Nucl. Part. Sci. **43**, 379 (1993).
[5] J. Richert and P. Wagner, Phys. Rep. **350**, 1 (2001).
[6] J. B. Natowitz, R. Wada, K. Hagel, T. Keutgen, M. Murray, A. Makeev, L. Qin, P. Smith, and C. Hamilton, Phys. Rev. C **65**, 034618 (2002).
[7] J. B. Elliott *et al.*, Phys. Rev. C **67**, 024609 (2003).
[8] P. Chomaz, M. Colonna, and J. Randrup, Phys. Rep. **389**, 263 (2004).
[9] S. K. Samaddar, J. N. De, and A. Bonasera, Phys. Rev. C **71**, 011601(R) (2005).
[10] L. P. Remsberg and D. G. Perry, Phys. Rev. Lett. **35**, 361 (1975).
[11] D. R. Fortney and N. T. Porile, Phys. Rev. C **14**, 1652 (1976).
[12] D. R. Fortney and N. T. Porile, Phys. Rev. C **21**, 2511 (1980).
[13] N. T. Porile *et al.*, Phys. Rev. Lett. **43**, 918 (1979).
[14] J. Hüfner and H. M. Sommermann, Phys. Rev. C **27**, 2090 (1983).
[15] W. Bauer, G. F. Bertsch, and H. Schulz, Phys. Rev. Lett. **69**, 1888 (1992).
[16] Y. Hirata, A. Ohnishi, Y. Nara, T. Kido, T. Maruyama, N. Otuka, K. Niita, H. Takada, and S. Chiba, Nucl. Phys. **A707**, 193 (2002).
[17] A. LeFèvre *et al.*, Nucl. Phys. **A735**, 219 (2004).
[18] W.-C. Hsi *et al.*, Phys. Rev. C **58**, R13 (1998).
[19] W.-C. Hsi *et al.*, Phys. Rev. C **60**, 034609 (1999).
[20] R. W. Stoenner, P. E. Haustein, and J. B. Cumming, Phys. Rev. Lett. **53**, 341 (1984).
[21] J. B. Cumming, P. E. Haustein, and R. W. Stoenner, Phys. Rev. C **33**, 926 (1986).
[22] W. Loveland, K. Aleklett, M. Bronikowski, Y. Y. Chu, J. B. Cumming, P. E. Haustein, S. Katcoff, N. T. Porile, and L. Sihver, Phys. Rev. C **37**, 1311 (1988).
[23] S. Pandian and N. T. Porile, Phys. Rev. C **23**, 427 (1981).
[24] S. B. Kaufman, E. P. Steinberg, and M. W. Weisfield, Phys. Rev. C **18**, 1349 (1978).
[25] J. S. Stewart and N. T. Porile, Phys. Rev. C **25**, 478 (1982).
[26] N. T. Porile *et al.*, Phys. Rev. C **39**, 1914 (1989).
[27] M. V. Ricciardi *et al.*, Phys. Rev. C **73**, 014607 (2006).
[28] T. Murakami and K. H. Tanaka, Nucl. Phys. **A734**, E96 (2004).